

## Vessel Size Imaging in the Brainstem

Michael Germuska<sup>1</sup> and Daniel Bulte<sup>1</sup>

<sup>1</sup>Nuffield Department of Clinical Neurosciences, University of Oxford, Oxford, Oxfordshire, United Kingdom

### Introduction

Imaging biomarkers are increasingly being used to evaluate novel therapeutics and targets in oncology. One such biomarker that shows promising results is MRI measurement of vessel size. A number of pre-clinical studies<sup>1,2,3</sup> have shown a strong correlation with histological measurements and response to treatment. In recent years, a variant of vessel size imaging (VSI) that uses an evoked BOLD response (using gas challenges) has been demonstrated in the human brain<sup>4,5</sup>. This new technique offers a completely non-invasive method of evaluating disease and treatment in a clinical setting. Here we investigate the possibility of acquiring BOLD-VSI data in the brainstem, which is the location of 10% of childhood brain tumors<sup>6</sup>. As with standard fMRI studies, data from the brainstem is highly influenced by cardiogenic noise. Two different data acquisition methodologies: dual-echo EPI (gradient/spin) and multi-echo single-shot-sampling of spin-echo refocusing (MESSER), are compared with and without cardiac gating. The initial results demonstrate an increase in performance for both gated acquisitions (against their respective continuous acquisitions), each demonstrating a significant reduction in chi-square fitting residuals. While the dual-echo readout demonstrably outperforms the MESSER acquisition both with and without cardiac gating.

### Theory

VSI is based on the vessel size dependence of  $T_2$  and  $T_2^*$ -weighted acquisitions. Changes in susceptibility during breathing challenges result in differential changes in  $T_2$  and  $T_2^*$ -weighted signals, from which estimates of mean vessel radius can be made using appropriate biophysical models<sup>4</sup>. During data acquisition the brainstem is subject to cardiac noise due to the basilar artery and natural elongation and contraction of the whole brainstem. Gated acquisitions have been shown to significantly reduce this noise<sup>7</sup>, but result in temporal fluctuations in signal due to the changing repetition time (TR). Fitting to multi-echo acquisitions can overcome these fluctuations, creating purely  $T_2$  or  $T_2^*$ -weighted images. In this study a MESSER acquisition is used with 3 EPI readouts either side of a refocusing pulse. The first three echoes (free-induction decay) are used to calculate  $R_2^*$ , while the second set of echoes (spin-echo re-phasing) are used to calculate  $R_2$  as per Jochimsen et al<sup>9</sup>, where  $R_2 = (R_2^* + R_2^*)/2$ . Alternatively, single echo data can be corrected for the temporal signal changes with a  $T_1$  map. Here we estimate  $T_1$  from the GE readout according to the method outlined by Guimaraes et al<sup>8</sup>, minimising the function  $S_{(n,i)}[1 - \exp(-TR_i/T_{1,n})]^{-1}$  during signal plateau periods (where  $S_{(n,i)}$  is the measured signal and  $TR_i$  is the repetition time for each readout).

### Methods

Two healthy volunteers were scanned on a 3 Tesla Siemens Verio with a 32-channel head coil. For each subject a diffusion weighted scan (3 orthogonal directions with two b values (0 and 1000mm<sup>2</sup>/s)) and four VSI scans were acquired. The VSI data was acquired using a dual GE-SE EPI readout (TR=2s, TE=30/90ms) and a MESSER EPI readout (TR=2s, TE=13,31,49,78,95,113ms Spin Echo time=125ms). A GRAPPA factor of 2 was used for both readouts. Thirteen axial slices (3.1x3.1x4mm voxels, 1.0mm inter-slice gap) were acquired with and without cardiac gating. Each VSI imaging paradigm consisted of one 18-minute session, comprised of 3x3minute hyperoxic periods interleaved with 3x3minute periods of normal air. During periods of hyperoxia, 100% oxygen was delivered to the volunteers via a non-rebreathing mask. All individual echoes were motion corrected and spatially smoothed (8mm FWHM) with FSL. A 2<sup>nd</sup> order time domain filter was then used to further reduce noise (this was applied to the MESSER data after relaxation rate calculation to maintain any baseline drift and  $T_1$  dependence between echoes). Dual-echo data was high-pass filtered to remove baseline changes. The MESSER data was fit with a linear regression to produce  $\Delta R_2$  and  $\Delta R_2^*$  data. Relaxation rate changes for the dual echo data were calculated as  $\Delta R_2^* = -\log(S_{GE}(t)/S_{0,GE})/TE_{GE}$  and  $\Delta R_2 = -\log(S_{SE}(t)/S_{0,SE})/TE_{SE}$ . The plateau periods from the triggered GE data (with TR times calculated from DICOM headers) were used to estimate  $T_1$  maps, and correct for variations in TR. A weighted total least squares regression was used to calculate q, the ratio of  $\Delta R_2^*$  and  $\Delta R_2$ . q values were masked, limited to a range of 1 to 25 and converted to mean vessel radii via a polynomial fit to Monte-Carlo model data (using the group mean ADC value of 0.753 $\mu$ m<sup>2</sup>/ms and an assumed susceptibility change of 0.2ppm).

### Results

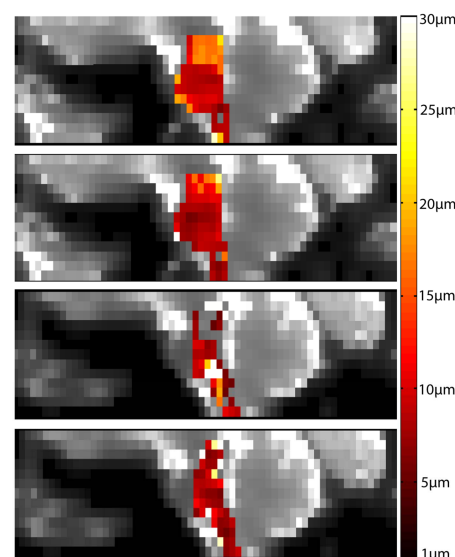
The figure shows example vessel size maps calculated with each acquisition method. The group averaged brainstem values and fitting residuals are given in the table below. The dual-echo gated sequence appears to provide the most accurate estimates of vessel size, producing the smallest chi-square fitting residuals (mean chi-square/DOF<0.5). The figure clearly illustrates the superiority of the gated MESSER acquisition compared to a continuous acquisition. However, neither MESSER sequence is able to produce robust estimates in the Pons. The mean vessel size estimate made with the gated dual-echo acquisition, 9.3  $\mu$ m, is lower than the majority of previous gray matter measurements<sup>4,10,11</sup>. This is consistent with the lack of large (draining) veins in the brainstem, and similar to measurements made in the thalamus<sup>11</sup>.

### Discussion and Conclusions

The increased performance of the gated acquisitions is consistent with previous results in brainstem fMRI<sup>7</sup> and further demonstrates the robustness of  $T_1$  estimates from gated EPI data. The inability for the MESSER sequence to make robust vessel size estimates in the Pons is likely due to the large susceptibility gradient in the anterior aspect of the brainstem, the short  $T_2^*$  in this region causing considerable attenuation of the signal in the 4<sup>th</sup> echo readout. The noise associated with fitting  $R_2^*$  is also the likely cause of the poor performance of the multi-echo data. The robust fits produced by the gated dual-echo acquisitions suggest that this methodology can become a useful tool for assessing vascular changes in the brainstem.

### References

1. Walker-Samuel S, et al. Int. J. Cancer 2012;(130):1284-1293.
2. Farrar C, et al. Neuro-Oncology 2010;(12):341-350.
3. Lemasson B, et al. Magn Reson Med 2012 Epub 24218 .
4. Jochimsen TH, et al. Neuroimage 2010;(51):765-774.
5. Shen Y, et al. Neuroimage 2011;(55):1063-1067.
6. cancer.net/cancer-types/brain-stem-glioma-childhood/statistics (05/11/2012)



Example vessel size maps ( $\mu$ m) for each method. From top to bottom: dual-echo continuous acquisition, dual-echo gated, MESSER continuous, MESSER gated.

	q	Vessel Radius ( $\mu$ m)	Chi-square/DOF
GE/SE	3.11 $\pm$ 0.87	10.0 $\pm$ 3.0	0.96 $\pm$ 0.62
GE/SE Gated	2.94 $\pm$ 1.15	9.3 $\pm$ 3.6	0.46 $\pm$ 0.29
MESSER	4.28 $\pm$ 5.66	13.2 $\pm$ 17.1	1.82 $\pm$ 1.05
MESSER Gated	3.68 $\pm$ 4.26	10.6 $\pm$ 13.0	1.19 $\pm$ 0.74

Mean brainstem vessel radii ( $\mu$ m), q values and fitting residuals for each acquisition method

7. Zhang WT, et al. Neuroimage 2006;(31):1506-1512.
8. Guimaraes TD, et al. Hum. Brain Mapp 1998;(6):33-41.
9. Jochimsen and Moller. Neuroimage 2008;(40):228-236.
10. Kiselev VG, J. Magn. Reson. 2005;(22):693-696
11. Xu C, et al. J. Cerebral Blood Flow & Metablosim 2011;(31):1687-1695.